HHS Public Access

Author manuscript

Acad Radiol. Author manuscript; available in PMC 2018 October 01.

Published in final edited form as:

Acad Radiol. 2017 October ; 24(10): 1240–1255. doi:10.1016/j.acra.2017.03.020.

Optical Mammography in Patients with Breast Cancer Undergoing Neoadjuvant Chemotherapy: Individual Clinical Response Index

Pamela G. Anderson[a], **Sirishma Kalli**[b], **Angelo Sassaroli**[a], **Nishanth Krishnamurthy**[a], **Shital S. Makim**[b], **Roger A. Graham**[c], and **Sergio Fantini**[a]

[a]Tufts University, Department of Biomedical Engineering, 4 Colby Street, Medford, MA 02155

[b]Tufts Medical Center, Department of Radiology, 800 Washington Street, Boston, MA 02111

[c]Tufts Medical Center, Department of Surgery, 800 Washington Street, Boston, MA 02111

Abstract

Rationale and Objectives—We present an optical mammography study that aims to develop quantitative measures of pathologic response to neoadjuvant chemotherapy (NAC) in patients with breast cancer. Such quantitative measures are based on the concentrations of oxy-hemoglobin ($[HbO_2]$), deoxy-hemoglobin ([Hb]), total hemoglobin ([HbT]), and hemoglobin saturation (SO_2) in breast tissue at the tumor location and at sequential time-points during chemotherapy.

Materials and Methods—Continuous-wave, spectrally resolved optical mammography was performed in transmission and parallel-plate geometry on ten patients prior to treatment initiation and at each NAC administration (mean number of optical mammography sessions: 12; range: 7–18). Data on two patients were discarded for technical reasons. Patients were categorized as responders (>50% decrease in tumor size), or non-responders (<50% decrease in tumor size) based on imaging and histopathology results.

Results—At 50% completion of the NAC regimen (therapy midpoint), responders (6/8) demonstrated significant decreases in SO_2 (−27% ± 4%) and [HbT] (−35 ± 4 μM) at the tumor location with respect to baseline values. By contrast, non-responders (2/8) showed non-significant changes in SO_2 and [HbT] at therapy midpoint. We introduce a cumulative response index (CRI) as a quantitative measure of the individual patient's response to therapy. At therapy midpoint, the SO_2-based CRI had a sensitivity of 100% and a specificity of 100% for the identification of responders.

Conclusion—These results show that optical mammography is a promising tool to assess individual response to NAC at therapy midpoint to guide further decision making for neoadjuvant therapy.

Corresponding author: Sergio Fantini – Sergio.fantini@tufts.edu.

Keywords

Optical mammography; Near-infrared spectroscopy; Breast cancer; Neoadjuvant therapy

INTRODUCTION

Neoadjuvant chemotherapy

Neoadjuvant chemotherapy (NAC) is administered to patients prior to surgery in an effort to reduce the primary tumor size, whereas adjuvant chemotherapy is administered following surgery in an effort to reduce the risk of residual disease and cancer recurrence. A patient's response to NAC may be assessed by physical exam or breast imaging (clinical response), or by histology post-surgery (pathologic response) [1, 2]. Assessing response to neoadjuvant treatment is crucial, as a pathologic complete response (pCR), defined by having no residual carcinoma in the resected breast tissue and in axillary lymph nodes, has been associated with improved survival [2–5]. Strictly defined, pCR requires the absence of invasive tumor in the resected specimen, although some clinicians use the more restrictive requirement of no residual invasive or *in situ* disease [3]. Because of the better outcome associated with pCR, finding tools that can define the individual clinical response during the course of therapy and accurately predict pathologic response would be of great benefit. This is also true in patients with poor response to treatment, as early identification of this problem may allow the physician to alter the chemotherapy regimen to avoid disease progression and to identify a more effective chemotherapy option.

Imaging modalities under investigation to monitor therapy response

Imaging methods sensitive to functional tissue changes are being investigated for monitoring breast cancer patients' response to neoadjuvant chemotherapy. Functional tumor changes are of particular interest due to the limitations of structural assessment of tumor response based on physical examination, ultrasound imaging, or mammography [6]. Current imaging methods used to assess clinical response are via a decrease in the standard uptake value (SUV) of 18-fluorodeoxyglucose (^{18}F-FDG) by positron emission tomography-computed tomography (PET/CT) [7, 8], or a decrease in tumor size by contrast-enhanced magnetic resonance imaging (MRI) [7, 8]. Both of these methods, however, are expensive and invasive, as PET/CT requires injection of a radiopharmaceutical, and MRI requires injection of gadolinium-based contrast. Furthermore, the appropriate timing and frequency for assessing clinical response have not been established, and studies thus far have typically imaged at a single time point during therapy [7, 8].

Optical mammography utilizes light in the wavelength range of 650–1000 nm to sense the absorption and scattering properties of breast tissue. Diffuse optical imaging techniques have intrinsically low spatial resolution (on the order of 1 cm); however, this is not a limiting factor in a study on patients undergoing NAC, as they often have large palpable tumors that are several centimeters in size. Functional tissue information can be obtained by recovering the concentrations of oxy-hemoglobin, deoxy-hemoglobin, water, and lipids (denoted in the text as [HbO_2], [Hb], [H_2O], and [lipid], respectively) based on the wavelength-dependent absorption of light in breast tissue [9]. Scattering amplitude and scattering power can also be

measured, which relate to the size and density of the scattering centers in tissue [9]. Optical breast imaging approaches have been developed using a handheld probe for diffuse reflectance measurements [10–17], a circular arrangement of optical fibers around the pendulous breast [18–21], or a parallel plate, planar geometry for transmission measurements on the mildly compressed breast [22–29]. Quantification of breast tissue optical properties may be performed using homogeneous models [10, 12, 14, 15, 17, 24], which yield average measurements over the interrogated tissue volume, or perturbation approaches [23, 29] and tomographic reconstructions [11, 13, 16, 20–22, 25–28]which yield spatially resolved measurements. Homogeneous models are not able to accurately recover the localized tumor properties because they provide overall optical properties of the probed breast volume, which may be comprised of both cancerous and healthy tissue. However, the approach based on homogeneous models benefits from being robust against measurement errors and able to provide fewer, but more reproducible, parameters; these are two important features for a longitudinal study where patients are imaged at multiple time points during neoadjuvant chemotherapy.

Following initial case studies that first demonstrated the optical approach [17, 30, 31] [31], several groups have investigated optical methods to assess response to treatment in patients with breast cancer undergoing neoadjuvant therapy. Studies aiming to predict therapeutic response early in the treatment have shown significant differences between responders and non-responders one day [14] or one week [12, 27, 32, 33] after the start of therapy. Other studies report the response during the course of treatment, typically using 3–8 measurement time points, to determine if and when different therapeutic response levels can be distinguished during NAC [13, 15, 16, 20, 21, 26, 28, 34–37]. The primary focus of these studies has been on the chromophore concentrations measured at the tumor location over time, but some work has also focused on exploring the correlation between baseline, pre-treatment optical measurements and the level of response to NAC [16, 21, 38, 39]. More recently, dynamic optical measurements have been reported to discriminate responders and non-responders on the basis of the breast tissue hemodynamic response to breath holding [36] or breast compression [40]. Table 1 lists the published studies, in chronological order, of optical mammography in neoadjuvant chemotherapy; it reports the number of subjects, number of imaging sessions, duration, and major findings for each study. The last row in Table 1 refers to our study reported in this article.

Studies that used the baseline tumor properties (before chemotherapy starts) as the reference to which all sequential measurements (during chemotherapy) are compared have found significant differences between responders and non-responders one or four weeks after the start of chemotherapy [26, 27] and after the first cycle of chemotherapy [16, 21, 28]. In a study on ten patients, Soliman *et al.* reported that at four weeks into chemotherapy, responders have a significantly greater decrease in [Hb], [HbO_2], and scattering power compared to non-responders using tomographic reconstructions [26]. Adding an additional five patients to the analysis performed by Soliman *et al.*, Falou *et al.* examined a total of fifteen patients and found significant differences between the response groups at week 1 by examining the average properties taken over the entire cancerous breast (as opposed to just the tumor volume as previously done) [27]. Using the whole breast volume approach, [Hb] and [H_2O] were found to be the best predictive parameters for distinguishing response to

treatment, with both [Hb] and [H_2O] increasing in responding patients and decreasing in non-responders [27]. Obtaining measurements using a handheld probe and applying tomographic reconstructions, Zhu *et al.* performed a study on thirty-two patients undergoing neoadjuvant chemotherapy and found that, after the first treatment cycle, the responding patients had a significantly larger decrease in total hemoglobin concentration ([HbT]) compared to non-responders [16]. Jiang *et al.* measured nineteen patients with a circular arrangement of optical fibers around the pendulous breast and found a significantly larger drop in [HbT] for pCR patients compared to an increase in [HbT] for incomplete responders within the first cycle of chemotherapy [21]. In another study on twenty-two patients using a parallel plate, planar geometry, Schaafsma *et al.* also found significant differences in response groups after the first cycle of chemotherapy, where responding patients showed a decrease in [HbO_2] and non-responders exhibited an increase in [HbO_2] [28]. When monitoring patients throughout the duration of therapy, hemoglobin parameters seemed to best differentiate response groups. In particular, as can be seen in Table 1, a consistent response to NAC is a decrease in the concentration of hemoglobin (often separated into the two components of oxy- and deoxy-hemoglobin) at the tumor location [12, 13, 15–17, 20, 21, 26, 28, 30–34, 36, 37, 41].

Research plan for this study

Our optical mammography study was designed to image patients more frequently than in previous studies, and to report the results of the optical measurements at each of the imaging sessions. We collected optical mammograms at baseline (prior to NAC) and each time the patient received a chemotherapy infusion - ranging from a minimum of 7 to a maximum of 18 individual time points throughout the NAC regimen. As a point of reference, the majority of studies reported in the literature measure patients 3–8 times throughout treatment (see Table 1). A notable exception is a case study, where optical measurements were performed 19 times during the course of NAC in a single subject who had a partial pathological response [41].

By collecting and reporting frequent optical measurements in this study, we aimed to achieve two objectives: first, to provide a more detailed characterization of the time evolution of chromophore concentrations in breast tissue during neoadjuvant chemotherapy which can be used to identify optimal approach and timing to predict pathologic response; second, to obtain indications on the reliability of the measured optical parameters on the basis of their intra-patient variance over the longitudinal measurements over the 20–30 weeks of neoadjuvant chemotherapy treatment. Our main objective was to develop a quantitative index of the level of individual response to NAC.

MATERIALS AND METHODS

Optical imaging of patients with breast cancer

This study was approved by the Institutional Review Board of the Tufts Medical Center, and it was also compliant with the Health Insurance Portability and Accountability Act. Any woman over the age of 21 who was diagnosed with invasive breast cancer and scheduled to undergo neoadjuvant chemotherapy was eligible for this study. All patients read and signed

an informed consent before participating. Ten patients undergoing neoadjuvant chemotherapy were imaged in this study. The patients will be referred to as neoadjuvant chemotherapy patients using the acronym “NACP,” followed by an index number ranging from 1 to 10. Relevant information about each patient enrolled is shown in Table 2. Patient recruitment took place from September 2014 to December 2015. Optical mammograms were obtained on both breasts 2–27 days before the treatment began (baseline measurement) and each time the patient underwent a chemotherapy infusion (the frequency and number of infusions are detailed in Table 2). For each measurement session the right breast was always imaged first. Figure 1 shows the chemotherapy schedule (specifying the corresponding drugs administered) for all ten patients in the study. To compare the effects of treatment across patients, each infusion time point was converted from week No. to “percentage of therapy complete” to normalize for the length of treatment (which ranged from 18 to 22 weeks). The breast cancer subtypes in our study are also reported for all patients in Table 2: (1) positive for human epidermal growth factor receptor 2 (HER2+), (2) positive for estrogen receptors (ER) and negative for HER2 (ER+/HER2−), (3) negative for ER, progesterone receptors (PR), and HER2 (triple-negative breast cancer, TNBC) [7]. Four patients were premenopausal (NACP #1, 5, 7, 9), but chemotherapy caused a break in menstruation for all of them.

A continuous-wave optical mammography instrument was used to image the patients receiving neoadjuvant chemotherapy. This instrument is described in detail in our previous work [42], and here we report its relevant features. Either a xenon arc lamp (Model No. 6258; Newport Corporation, Irvine, CA, for NACP ## 1–5) or a quartz tungsten halogen lamp (Model No. 66997; Newport Corporation, Irvine, CA, for NACP ## 6–10) served as the light source, with its optical emission spectrally filtered to pass the wavelength range 500–1,000 nm. An illumination optical fiber and a collection optical fiber scan collinearly in transmission geometry over two parallel polycarbonate plates that mildly compress the breast. The detected light is spectrally dispersed by a spectrograph (Model No. SP-150; Princeton Instruments, Acton, MA) and measured by a cooled charge-coupled device (CCD) camera (Model No. DU420A-BR_DD; Andor Technology, South Windsor, CT). Transmission optical data through the breast were acquired spatially every 2 mm in the x and y directions and with a wavelength resolution of 8 nm over the spectral band of 650–850 nm. The time to scan one breast for each patient ranged from 3–10 min (average: 6 min) based on breast size. Each measurement session, including setup time and optical imaging of both breasts took 15–30 min.

Lab parameters and response categories

A complete blood count was obtained for every patient before each chemotherapy infusion and the hemoglobin concentration in blood (denoted at Hgb) was recorded. Since [HbT], the concentration of hemoglobin in tissue, is equal to the product of Hgb times the blood volume (i.e. the blood-to-tissue volume fraction), the Hgb data were used to translate [HbT] changes into blood volume changes. Specifically, the relative change in blood volume is given, to a good approximation, by the relative change in [HbT] minus the relative change in Hgb. This approach is important to separate the systemic effects of varying Hgb from the local effects of varying tissue vascularization on the measured [HbT] changes [17]. The relative blood

volume change with respect to the first chemotherapy infusion was determined for each patient throughout the course of treatment.

The response categories used in this work were determined from the tumor size pretreatment (with imaging) and post-treatment (from the pathology report based on histology following surgical excision/mastectomy). The two response categories are as follows:

1. Responders (R): Under this category, we include those patients who show a pathologic complete response (pCR) or a partial response 1 (PR1) (defined as any remaining tumor that had decreased by more than 50% in the maximum dimension, regardless of nodal status). The patients in the pCR and PR1 categories are both considered to be associated with an improved prognosis and thus were grouped together in the R category.
2. Non-responders (NR): Under this category, we include those patients who show a partial response 2 (PR2) (defined as any tumor that decreased by less than 50% in the maximum dimension, regardless of nodal status). This categorization, in agreement with Roblyer *et al.* [14], considers that patients whose tumor size decreased by less than 50% may have a less favorable prognosis.

From a clinical point of view, it is desirable to identify poorly responding tumors early in the NAC treatment period to help make changes to treatment protocols and maximize the therapeutic effects. Accordingly, we aim to identify R and NR patients during therapy based on optically measured parameters over the course of NAC.

It is worth pointing out that some ambiguity exists in the identification of responders and non-responders. First, the choice of 50% as the minimum reduction in tumor size for responders is somewhat arbitrary. Second, a classification solely based on tumor size may not properly take into account microscopic responses at the cellular level, as done by the five-point, Miller-Payne histological grading system [43]. This cellularity-based grading system of pathologic response (ranging from 1: no response, to 5: complete pathologic response) was used in some optical studies. However, even this method leads to some ambiguity, as shown by different groupings of the Miller-Payne grades. Zhu et al. considered grades 1–3 for non-responders and partial responders, and grades 4–5 for near-complete and complete responders [16]. By contrast, Schaafsma et al. considered grade 1 for non-responder and grades 2–5 for (partial) responders [28]. In some cases, criteria based on residual tumor size and decrease in cellularity were combined in the categorization of complete response, good pathologic response, or minimal pathologic response. A breast response index for continuous-scale assessment of NAC response (from 0: “no response” to 1: “pCR of both breast and axilla”) was also introduced on the basis of a change in T stage before and after treatment [44]. Ultimately, the goal of any assessment tool of clinical response is to identify, as early as possible in the course of NAC treatment, those patients who will have a poor clinical outcome with the ongoing treatment regimen. The classification considered by us achieves this goal because the NR patients, as defined above, are those who have a less favorable prognosis, and for which a change in treatment may be beneficial. On the other hand, although the goal of pCR is always desired, a partial response

which is close to pCR is also favorable, and thus both categories were considered as R patients.

Data Processing

A continuous-wave optical diffusion model for a homogeneous, infinite slab geometry was used to process the optical transmission spectra in the wavelength range 650–850 nm [45] and further details on the model implementation can be found in prior work [42]. Briefly, the model inputs at each pixel were the measured transmittance spectrum (over the full wavelength band 650–850 nm) and an estimate of the tissue thickness [46]. An inversion procedure based on the Levenberg-Marquardt method [47] was applied to directly recover the concentrations of HbO_2, Hb, water, and lipids by utilizing their known extinction spectra [48]. Since only continuous-wave light was used, the scattering properties were not measured and were set in order to recover unique chromophore concentrations [49]. There have been a few studies that measured scattering properties, and mixed results have been reported on the scattering contrast featured by breast cancer [9]. Therefore, the scattering amplitude and power ($\mu_s'(\lambda_0)$ and b, which represent the magnitude and the wavelength dependence of scattering, respectively) were fixed to values derived from results in the literature ($\mu_s'(\lambda_0 = 670\ \text{nm}) = 10.5\ \text{cm}^{-1}$, $b = 1$) [23]. Two additional optical parameters being reported in this study are total hemoglobin concentration ([HbT]) and hemoglobin saturation (SO_2). Hemoglobin saturation is the ratio of [HbO_2] to [HbT], a quantity representative of the balance between oxygen supply and the oxidative metabolic rate in tissue. The initial tumor location was identified in the cranio-caudal view X-ray mammogram, and a rectangular region including the tumor location was considered in the baseline [Hb] optical mammogram. The tumor region of interest (ROI) was defined as the collection of pixels within the rectangular region having [Hb] values greater than 75% of the maximum [Hb] value within the rectangular region [42]. We found that the specific threshold value (75% in this study) used to define the tumor ROI does not have a significant impact on the results reported in this manuscript. The placement and size of the tumor ROI was kept consistent for all sequential optical mammograms, by maintaining the distance of the ROI from the proximal and lateral edges of the breast. For each measurement session over the course of neoadjuvant chemotherapy, we compute the value of the optical parameters at the tumor ROI and the associated errors as the average and standard deviation, respectively, over all the pixels within the tumor ROI defined above.

Due to the homogenous tissue model being applied in this work, we observe that the recovered chromophore concentrations in the cancerous region represent contributions from both the tumor and healthy surrounding tissue. Since the tumors of NAC patients are typically large, the tissue being measured within the tumor ROI is mostly representative of cancerous tissue at baseline and at the start of treatment. However, if the patient responds to the treatment and the tumor shrinks, healthy tissue will contribute more and more to our optical measurements in the tumor ROI during the course of neoadjuvant chemotherapy. This is an important aspect to keep in mind for the interpretation of our results.

Two cases, NACP #1 and NACP #10, had to be discarded for technical reasons, since their tumor ROIs fell outside of the optical field of view in a number of imaging sessions as a

result of the tumor proximity to the chest wall. We point out that even though the tumor sizes determined by MRI and X-ray mammography are quite large (9.4 cm for NACP #1, 4.5 cm for NACP #10), the size of the tumor ROI identified in the optical mammograms, on the basis of the optical contrast provided by [Hb], is significantly smaller (1.2 cm for NACP #1, 1.9 cm for NACP #10).

The [H_2O] and [lipid] data were found to not provide reliable longitudinal results, which is likely attributed to the spectral range of 650–850 nm not being highly sensitive to those chromophores. Specifically, we found that there was a lack of a consistent trend (decreasing or increasing) in the percent change of [H_2O] and [lipid] from the baseline measurement for most patients. The frequency of the optical mammograms throughout the duration of therapy allows us to assess the variance and reliability of the observed trends in the optical parameters during neoadjuvant therapy.

Statistical analysis

Because of the relatively small number of patients analyzed in this study (8 of the 10 enrolled patients), we used a non-parametric Wilcoxon rank-sum test (with $p<0.05$ to indicate significance) to determine when responders (R) could be discriminated from non-responders (NR) on the basis of optical parameters at the tumor ROI. The statistical analysis was performed with MATLAB (Mathworks, Natick, MA). Grouping together pCR and PR1 patients into the R category is in line with the primary goal of this work, which is to evaluate whether and when NR can be distinguished from R. However, further stratifying R into pCR and PR1 may be beneficial for better assessing those patients in need of treatment changes, and this option will be considered in future studies on larger patient populations.

RESULTS

Patient Measurements

Representative breast images for a R (pCR) patient (NACP #5) are shown in Figure 2, which shows the full-field digital mammogram, the axial contrast-enhanced subtraction MRI image and the optical maps of [HbT] and SO_2 throughout NAC treatment. The outer 1 cm of the breast map is cut in the optical images due to the confounding contributions of edge effects in the optical data collected in the proximity of the breast edge. The rectangular region containing the tumor is shown in the X-ray image. The corresponding area is also shown in the optical mammograms at week 0 (dotted line) together with the tumor ROI (solid line) obtained from the [Hb] map as described in the methods section.

The decrease in [HbT] and SO_2 throughout the course of chemotherapy within the tumor ROI is apparent in Figure 2. The decrease in [HbT] at the tumor ROI during treatment is expected for a responder, since breast cancer has a greater [HbT] than surrounding healthy tissue [9–11]. However, the decrease in SO_2 at the tumor ROI may be somewhat surprising, especially considering our previous report of a lower SO_2 in breast cancer compared to healthy tissue [42]. As we will further discuss in the discussion section, a longitudinal study during NAC treatment must take into proper consideration the systemic effects of therapy.

We computed the mean value and standard error of the percent change from the baseline measurement (i.e. from before the start of NAC) for [Hb], [HbO_2], [HbT], and SO_2 at the tumor region of interest for each response group. The average percent changes over five binned temporal windows in the normalized time axis (defined in the materials and methods section) are reported in Table 3, which shows the response category in the first column, the five binned temporal windows in the second column, and the response to therapy at the tumor ROI in the third to sixth columns. From the definitions of [HbT] ([Hb]+[HbO_2]) and SO_2 ([HbO_2]/[HbT]), it follows that the relative change in [HbT] is a weighted average of the relative changes in [HbO_2] and [Hb] with weights given by the baseline values of SO_2 and (1-SO_2), respectively. Each bin is identified by the center point of its time interval (10%, 30%, 50%, 70%, or 90%) and the bounds of each bin are shown. The single parenthesis indicates the percentage therapy complete that is not included in the bin, whereas the bracket represents the percentage point that is included in the bin. Given the duration of NAC in this study (18–22 weeks), the 10% bin corresponds to approximately the first 4 weeks of treatment.

Group results and the individual patient data of the percent change from baseline for the [HbT] in the tumor ROI are shown in Figure 3. Figure 3 shows a decreasing [HbT] in R's compared to a relatively constant [HbT] in NR's. To translate these changes in hemoglobin concentration into changes in blood volume fraction, one needs to take into account the fact that the hematocrit, thus the hemoglobin concentration in blood, is also affected by NAC. The average relative change throughout treatment in [HbT], hemoglobin concentration in blood, and blood volume fraction for all eight patients is shown in Figure 4. It is apparent from Figure 4 that, during NAC, the concentration of hemoglobin in blood (Hgb) decreases in all patients, both R's and NR's. By calibrating the [HbT] changes by the Hgb changes, it can be seen that blood volume features an initial decrease after the start of NAC and then stays relatively constant in patients classified as R, whereas it increases in patients classified as NR.

To provide an indication of how perfusion and metabolic demand may be altered in cancerous breasts with varying levels of response, the tumor region SO_2 changes are shown on a group level and for each individual patient in Figure 5. Figure 5 conveys that the SO_2 decrease in the cancerous region scales with the level of response, with responding patients featuring a larger SO_2 decrease compared to the non-responding patients.

A non-parametric Wilcoxon rank-sum test was applied at all considered therapy complete time windows to determine if there was a significant difference between the observed changes in the [Hb], [HbO_2], [HbT], and SO_2 of the tumor ROIs for responding and non-responding patients. The p values for this statistical test are reported in Table 4 and show that [HbO_2], [HbT], and SO_2 achieve a statistically significant discrimination ($p \leq 0.05$) of the R and NR groups at therapy midpoint and beyond. A p value of 0.06, marginally greater than the significance level, was observed at the 20–40% therapy complete window for [HbO_2], [HbT], and SO_2.

Cumulative Response Index

In an effort to move beyond a group analysis to assess individual patient response to NAC, we introduce a cumulative response index (CRI) at a single patient level. This CRI is calculated at each therapy session on the basis of the optical mammograms recorded at that session and all previous sessions, and thus it takes advantage of the cumulative information collected with optical mammography during the course of treatment. The CRI serves as an individual indicator for how the patient is responding and can take values between −1 (no response) and +1 (complete response). The CRI can be defined for any measured parameters of the tumor ROI ([Hb], [HbO_2], [HbT], SO_2, etc.). Here, to illustrate the CRI concept, we define the CRI in terms of SO_2. To start, we compute a threshold value for therapy response at each % therapy complete time window by taking the weighted average of the mean percent change of SO_2 for the R and NR group results, with weights given by the inverse of the standard error. In the case of SO_2, the R group and NR group results are reported in Figure 5 by the solid line and dashed line, respectively. Then, a linear interpolation is performed to create an SO_2 threshold line over the entire therapy period. This threshold line is taken to represent the boundary that separates SO_2 changes in responding and non-responding tumors. For each measurement session i, one can compute the difference d_i, as the threshold value of SO_2 minus the percent change of SO_2 at that particular time point (percentage of therapy complete). The standard deviation associated with d_i is denoted as $\sigma(d_i)$ and refers to the standard deviation across all pixels within the tumor ROI for the i-th imaging session. Subsequently, the CRI at the n-th session is defined as follows:

$$\mathrm{CRI(n)}=\frac{\sum_{\mathrm{i=1}}^{\mathrm{n}}\frac{\mathrm{d_i}}{\sigma(\mathrm{d_i})}}{\sum_{\mathrm{i=1}}^{\mathrm{n}}\frac{|\mathrm{d_i}|}{\sigma(\mathrm{d_i})}} \quad (1)$$

The normalization factor in the denominator of the right-hand-side of Eq. (1) limits the CRI values to the range [−1, +1]. When the SO_2 at a tumor ROI falls above the threshold line, its contribution to the CRI is negative, whereas when it falls below the threshold line its contribution to the CRI is positive. Therefore, positive CRI values are associated with responders, and negative CRI values are associated with non-responders.

The SO_2 cumulative response index was found for each patient. Figure 6 shows each patient's SO_2 CRI, and Table 4 reports the sensitivity and specificity for response classification achieved at different time points during therapy using the CRI associated with [Hb], [HbO_2], [HbT], or SO_2. The sensitivity and specificity were calculated by considering positive and negative values of the CRIs to represent R and NR, respectively (in other words, we have considered a threshold value of 0 to categorize R (positive CRI) and NR (negative CRI)). Of course, one may chose a different CRI threshold value or define a different threshold line during the course of treatment, and build a receiver operating characteristic (ROC) curve. However, given the limited patient population, the point of this study is to illustrate our proposed approach to the assessment of individual response to neoadjuvant therapy, a point that is made by the results reported in Figure 6 and Table 4.

Table 4 shows that the SO_2 CRI achieved the best NAC assessment results, with sensitivity/specificity of 83%/100% after 20% therapy complete, and 100%/100% after 40% therapy complete. Comparable results were achieved with [HbO_2] and [HbT], but they were marginally worse than the SO_2 results in this study.

DISCUSSION

[HbT] response to neoadjuvant chemotherapy at the tumor ROI

As shown in Table 1, a consistent result reported in the literature is the decrease of [HbT] at the tumor location during the course of NAC for patients who respond to therapy. In partial responders or non-responders, the tumor [HbT] was found to decrease by a smaller amount than in responders, or to remain either constant or increase slightly during NAC. Specifically, within the first four weeks of NAC, studies that included both responders and non-responders found that the [HbT] at the tumor location decreased by as much as 60% [12, 16, 20, 21, 28, 34, 36], whereas non-responders (or partial responders) showed a lesser decrease [26], no change [12, 16, 34, 36], or an increase [20, 21, 28] in [HbT] at the tumor location. In this study, we confirmed this result, having observed a reduction in [HbT] of about 30% in the tumor ROI for responding patients as opposed to a non-significant change in non-responding patients in the course of therapy (starting at 20% of therapy, i.e. about 4 weeks into NAC) (see Table 3).

Changes in tissue [HbT] are the result of either or both of two factors: a change in tissue vascularization (i.e. in the blood volume ratio) or a change in the concentration of hemoglobin in blood (i.e. in hematocrit). On the basis of Figure 4, our results in responders are assigned to a combination of both factors - a reduction (by about 15%) in the tumor vascular density, which has been previously reported [34], and a systemic decrease (by about 20%) in the hemoglobin concentration in blood (Hgb), resulting from NAC [50]. Because a comparable systemic decrease in Hgb was observed in responders and non-responders, our [HbT] results indicate that the tumors in non-responders feature an increased vascularization during the course of NAC (see Figure 4).

It is important to note that, in the case of patients who respond well to treatment, the tumor ROI contains more and more non-cancerous tissue during the course of treatment. Therefore, the decrease in [HbT] observed during NAC in responding patients represents NAC-induced changes in cancerous tissue (early in NAC) as well as in healthy tissue (later in NAC). By contrast, in the case of non-responders, for whom the tumor ROI always contains a significant amount of cancerous tissue, the [HbT] evolution during NAC is mostly representative of changes in cancerous tissue.

Because of the systemic effects of NAC as a result of the systemic decrease in Hgb, one would expect a systemic decrease in [HbT] throughout the body, and in particular in the contralateral, healthy breast (as also reported in [14, 17, 51]). We similarly observed a reduction in [HbT] in the contralateral, healthy breast, to a different extent in responders and non-responders, suggesting that systemic effects of NAC in peripheral tissue may also be indicative of the level of therapeutic response.

SO_2 response to neoadjuvant chemotherapy at the tumor ROI

It is somewhat surprising that among all of the published studies only a few have reported results of the evolution of tumor SO_2 during the course of NAC. For example, the two pioneering case studies reported a tumor-to-normal SO_2 ratio of about 0.9 throughout NAC with an increase to 1.4 after the end of NAC [17] and a decrease in the tumor SO_2 after the 5^{th} NAC cycle from ~81% to ~60% [30]. In part, this paucity of SO_2 data in optical NAC studies may be due to the fact that several optical mammography studies have reported a lack of contrast provided by tumor SO_2 [9]. However, as noted at the end of the previous section, the combination of systemic and local effects of NAC may introduce new physiological and metabolic processes that differentiate responders and non-responders. In fact, in this study we found that the oxygen saturation of hemoglobin at the tumor ROI was the quantity most strongly associated with the level of patient response to neoadjuvant chemotherapy. At the tumor ROI, we observed a stronger decrease of SO_2 in responders (about −10% at 20–40% therapy complete, and about −30% throughout the rest of NAC) than in non-responders (a decrease of a few percent, significant only toward the end of NAC) (see Table 3). Furthermore, the SO_2 CRI achieved the best sensitivity and specificity for patient response assessment (see Table 4).

The physiological sources of decrease in tissue SO_2 are: (1) a decrease in tissue vascularization, associated with a regression of angiogenesis, (2) a decrease in blood flow, which reflects the local gradient in blood pressure as well as the compliance, reactivity (dilation/constriction), and architecture of the vasculature, and (3) an increase in the tissue metabolic rate of oxygen which relates to cellular metabolism. While breast cancer is typically associated with angiogenesis, perturbations to cellular metabolism and tissue perfusion, the specific angiogenic, metabolic, and perfusion responses to chemotherapy are not fully understood or characterized.

From a technical point of view, optical measurements of SO_2 are typically found to be robust since they rely on assessing concentration ratios ($[HbO_2]/[HbT]$) rather than absolute concentrations. To test the qualitative accuracy of our homogeneous tissue model approach, we have generated forward data for an inhomogeneous medium using a perturbation approach in diffusion theory [52]. When we set the SO_2 of the localized perturbation to be either lower or higher than that of the background medium, the recovered SO_2 value (using the homogeneous tissue model reported here) is always qualitatively correct, i.e. it accurately reflects the direction (higher or lower) of the localized SO_2 change from the background.

Results obtained using PET/CT techniques indicate a decrease in cellular metabolism when tumors respond to treatment due to the reduction in the absolute number of cancerous cells and in their proliferative activity [7, 53]. These results may appear to contradict our findings of decreasing SO_2 in responders. However, one needs to recall that cellular metabolism is only one factor affecting the hemoglobin saturation within the tumor location. Tissue perfusion is another critical factor, as it affects the rate of oxygen delivery to tissue. Using contrast enhanced MRI or [^{15}O]-water PET imaging, responding tumors have been found to show a significantly stronger decrease in perfusion compared to poorer responding tumors [54–57]. Therefore, our finding of a greater decrease of SO_2 in the tumor ROI of responding

patients is consistent with a dominant effect of the reduction in blood flow vs. the reduction in cellular metabolism.

We stress again that chemotherapy is not a localized treatment, and it will also impact the healthy tissue being measured in the optical mammograms. The direction of the response in the SO_2 of cancerous and healthy tissue depends on the relative magnitude of the changes in blood flow, oxygen consumption, and blood volume during treatment. The chemotherapy effects on the SO_2 of healthy tissue were observed in the contralateral, healthy breast, which showed stronger decreases (~45% in responders, and ~15% in non-responders, after midpoint) than the tumor ROI in the cancerous breast. This finding provides insight into how the healthy tissue responds to chemotherapy, and it explains the apparent inconsistency between the observed decrease of SO_2 in the tumor ROI of responders, and the previously reported lower SO_2 of cancerous tissue with respect to the surrounding healthy tissue (by −5±1%) [42]. In fact, one should expect responding tumors to feature an SO_2 value that approaches the SO_2 value of healthy tissue. In the absence of any systemic effects, this means that responding tumors should feature an *increase* in SO_2 during the course of NAC. However, in the presence of systemic effects that lower the SO_2 of healthy tissue to levels below the baseline SO_2 of cancerous tissue, responding tumors should indeed feature a *decrease* in SO_2. Furthermore, such decrease should be lower than that of healthy tissue, simply because of the lower baseline value of SO_2 in cancerous vs. healthy tissue. This is what we observed in our study and shows the importance of systemic effects of NAC in the interpretation of optical mammography data. Systemic effects of neoadjuvant chemotherapy should also be taken into account when considering tumor-to-normal (T/N) ratios, and whether the choice for a reference tissue should be a tissue area in the cancerous breast or in the contralateral breast.

Limitations of the study and future directions

The results reported in this work are limited by the small sample size of patients that we were able to enroll in the study. Because of the small sample size, the cumulative response index (CRI) was calculated on the basis of a threshold line computed from data collected on the same patients that were then classified with this method. In a larger study, the robustness of this method would be tested by only using a subset of the patient data to generate the criteria used to classify the rest of the patients. However, the results reported here do show the potential of optical mammography to discriminate responders and non-responders on an individual basis during the NAC regimen.

The limited statistical significance achievable with a small sample size is further exacerbated by the heterogeneous patient population, in terms of both the prescribed chemotherapy agents and the NAC duration and infusion frequency. However, we observe that optical mammography is sensitive to the end result of vascular, hemodynamic, and metabolic perturbations, regardless of the biological mechanisms that are responsible for them. Furthermore, the relatively large number of optical measurements reported in this study throughout treatment (ranging from a minimum of 7 to a maximum of 18, mean number: 12) shows their robustness as reflected by their progressive trends during NAC. Of course, optical mammograms can in principle be performed on a regular weekly or biweekly

schedule, independent of the NAC infusion schedule, thus providing a more regular and temporally refined monitoring of NAC response.

A key assumption of our approach is that the optical scattering properties of tissue are kept constant. This means that any changes in tissue scattering that may occur during chemotherapy are not considered. To test how changes in the scattering properties may impact the recovered chromophore concentrations and their corresponding trends throughout treatment, NACP #5 data at baseline, midpoint and end of therapy, were used with different set values of the reduced scattering coefficient and its wavelength dependence. There are limited tumor scattering parameters reported in neoadjuvant chemotherapy monitoring studies to guide our selection. The trend in scattering power (i.e. the wavelength dependence of scattering) considered by us was based on the percent changes at 4 weeks and pre-surgery reported by Soliman *et al.* [26]. The scattering amplitude (i.e. the absolute value of scattering) was then set to decrease by 10% at the therapy midpoint and by another 10% at the end of therapy. By fixing these decreasing scattering values, the trends in NACP #5 [Hb], [HbO_2], [HbT], and SO_2 were found to be all in the same direction, with magnitudes within one standard deviation of each point, compared to when the scattering parameters were fixed to the same value throughout therapy. Therefore, chemotherapy induced scattering property responses are unlikely to affect the chromophore concentration trends observed in this work.

The cancer-to-healthy-tissue contrast in the chromophore concentrations at baseline were examined to determine if the level of NAC response could be predicted before treatment began. This contrast measure was calculated at baseline in two different ways, as the difference between the average chromophore concentration at the tumor ROI and either the one at the healthy background tissue in the same breast or at the symmetrical region in the contralateral breast. The tumor contrast measured at baseline, however, was not able to distinguish response groups for this patient population.

With a larger sample size of patients, one may perform more refined statistical analyses, such as an ordinal logistic regression to determine which optical parameters at which time points are significantly different between R and NR groups. Additonally, a more stratified analysis of breast cancer subtypes, chemotherapy regimens, and response to therapy (i.e. partial vs. complete responders) may be performed. Since it has been reported that pCR is a more relevant endpoint for TNBC and HER2+ cases, one could determine if there are certain optical parameters that may serve as better outcome predictors for a given subtype.

CONCLUSIONS

Ten breast cancer patients receiving neoadjuvant chemotherapy were imaged at each treatment time point using broadband, continuous-wave, optical mammography. For eight of these ten patients, the tumor ROI fell within the field of view of the optical mammograms throughout NAC and were analyzed for discrimination of responders and non-responders. The time evolutions of [HbT], [HbO_2], and SO_2 at the tumor ROI during the course of therapy have been found to correlate with pathologic response. A cumulative response index (CRI), which may be based on any tumor parameter, was developed to assess how individual

patients respond throughout treatment. The best performance was obtained with the SO_2 CRI which achieved a 100% sensitivity and specificity at therapy midpoint and beyond.

To further confirm the clinical importance of early assessment of patient response to NAC, a published study reported a neoadjvuant chemotherapy trial where therapy was switched based on the initial clinical response as assessed by physical exam (palpation), ultrasound, and mammography at the end of the second NAC cycle [58]. By changing the therapy regimen for patients with a clinical poor response, the ER+/HER2− patients were found to have a significant improvement in disease free suvival [58]. A non-invasive, safe, and relatively simple imaging tool (like optical mammography) that can determine clinical response and also predict pathologic response can serve as a useful technique to assess the efficacy of NAC and allow for physicians to change treatment for non-responders.

Acknowledgments

We thank Cate Mullen, RN, for all her help, especially with recruiting patients for this study. We would also like to give a special thank you to the patients who participated in this research. This research is supported by the National Institutes of Health [grant number R01 CA154774]. This material is also based upon work supported by the National Science Foundation Graduate Research Fellowship [grant number NSF DGE-0806676]. Any opinion, findings, and conclusions or recommendations expressed in this material are those of the author(s) and do not necessarily reflect the views of the National Science Foundation.

Abbreviations

[Hb]	concentration of deoxy-hemoglobin
[HbO_2]	concentration of oxy-hemoglobin
[HbT]	concentration of total hemoglobin
CRI	cumulative response index
ER	estrogen receptors
ER+/HER2	positive for estrogen receptors and negative for human epidermal growth factor receptor 2
HER2+	positive for human epidermal growth factor receptor 2
Hgb	hemoglobin concentration in blood
MRI	magnetic resonance imaging
NAC	neoadjuvant chemotherapy
NACP	neoadjuvant chemotherapy patient
NR	non-responders
pCR	pathologic complete response
PET/CT	positron emission tomography-computed tomography
PR	progesterone receptors

PR1	partial response 1
PR2	partial response 2
R	responders
ROI	region of interest
SO_2	hemoglobin saturation
TNBC	triple-negative breast cancer

References

1. Mauri D, Pavlidis N, Ioannidis JPA. Neoadjuvant versus adjuvant systemic treatment in breast cancer: A meta-analysis. J Natl Cancer Inst. 2005; 97(3):188–194. [PubMed: 15687361]
2. Rastogi P, Anderson SJ, Bear HD, Geyer CE, Kahlenberg MS, Robidoux A, Margolese RG, Hoehn JL, Vogel VG, Dakhil SR, et al. Preoperative chemotherapy: updates of National Surgical Adjuvant Breast and Bowel Project Protocols B-18 and B-27. J Clin Oncol. 2008; 26(5):778–785. [PubMed: 18258986]
3. Von Minckwitz G, Untch M, Blohmer JU, Costa SD, Eidtmann H, Fasching PA, Gerber B, Eiermann W, Hilfrich J, Huober J, et al. Definition and impact of pathologic complete response on prognosis after neoadjuvant chemotherapy in various intrinsic breast cancer subtypes. J Clin Oncol. 2012; 30(15):1796–1804. [PubMed: 22508812]
4. Guarneri V, Broglio K, Kau S, Cristofanilli M, Buzdar AU, Valero V, Buchholz T, Meric F, Middleton L, Hortobagyi GN, et al. Prognostic value of pathologic complete response after primary chemotherapy in relation to hormone receptor status and other factors. J Clin Oncol. 2006; 24(7): 1037–1044. [PubMed: 16505422]
5. Gampenrieder SP, Rinnerthaler G, Greil R. Neoadjuvant chemotherapy and targeted therapy in breast cancer: Past, present, and future. J Oncol. 2013:732047. [PubMed: 24027583]
6. Chagpar AB, Middleton LP, Sahin AA, Dempsey P, Buzdar AU, Mirza AN, Ames FC, Babiera GV, Feig BW, Hunt KK, et al. Accuracy of physical examination, ultrasonography, and mammography in predicting residual pathologic tumor size in patients treated with neoadjuvant chemotherapy. Ann Surg. 2006; 243(2):257–264. [PubMed: 16432360]
7. Groheux D, Majdoub M, Sanna A, de Cremoux P, Hindié E, Giacchetti S, Martineau A, de Roquancourt A, Merlet P, Visvikis D, et al. Early Metabolic Response to Neoadjuvant Treatment: FDG PET/CT Criteria according to Breast Cancer Subtype. Radiology. 2015; 277(2):358–371. [PubMed: 25915099]
8. Loo CE, Straver ME, Rodenhuis S, Muller SH, Wesseling J, Vrancken Peeters MJTFD, Gilhuijs KGA. Magnetic resonance imaging response monitoring of breast cancer during neoadjuvant chemotherapy: Relevance of Breast Cancer Subtype. J Clin Oncol. 2011; 29(6):660–666. [PubMed: 21220595]
9. Fantini S, Sassaroli A. Near-infrared optical mammography for breast cancer detection with intrinsic contrast. Ann Biomed Eng. 2012; 40(2):398–407. [PubMed: 21971964]
10. Cerussi A, Shah N, Hsiang D, Durkin A, Butler J, Tromberg BJ. In vivo absorption, scattering, and physiologic properties of 58 malignant breast tumors determined by broadband diffuse optical spectroscopy. J Biomed Opt International Society for Optics and Photonics. 2006; 11(4):44005.
11. Zhu Q, Kurtzma SH, Hegde P, Tannenbaum S, Kane M, Huang M, Chen NG, Jagjivan B, Zarfos K. Utilizing optical tomography with ultrasound localization to image heterogeneous hemoglobin distribution in large breast cancers. Neoplasia. 2005; 7(3):263–270. [PubMed: 15799826]
12. Cerussi A, Hsiang D, Shah N, Mehta R, Durkin A, Butler J, Tromberg BJ. Predicting response to breast cancer neoadjuvant chemotherapy using diffuse optical spectroscopy. Proc Natl Acad Sci U S A. 2007; 104(10):4014–4019. [PubMed: 17360469]

13. Zhu Q, Tannenbaum S, Hegde P, Kane M. Noninvasive monitoring of breast cancer during neoadjuvant chemotherapy using optical tomography with ultrasound localization. Neoplasia. 2008; 10(10):1028–1040. [PubMed: 18813360]
14. Roblyer D, Ueda S, Cerussi A, Tanamai W, Durkin A, Mehta R, Hsiang D, Butler Ja, McLaren C, Chen W-P, et al. Optical imaging of breast cancer oxyhemoglobin flare correlates with neoadjuvant chemotherapy response one day after starting treatment. Proc Natl Acad Sci U S A. 2011; 108(35): 14626–14631. [PubMed: 21852577]
15. Cerussi AE, Tanamai VW, Hsiang D, Butler J, Mehta RS, Tromberg BJ. Diffuse optical spectroscopic imaging correlates with final pathological response in breast cancer neoadjuvant chemotherapy. Philos Trans A Math Phys Eng Sci. 2011; 1955; 369:4512–4530. [PubMed: 22006904]
16. Zhu Q, DeFusco PA, Ricci A, Cronin EB, Hegde PU, Kane M, Tavakoli B, Xu Y, Hart J, Tannenbaum SH. Breast cancer: assessing response to neoadjuvant chemotherapy by using US-guided near-infrared tomography. Radiology. 2013; 266(2):433–442. [PubMed: 23264349]
17. Jakubowski DB, Cerussi AE, Bevilacqua F, Shah N, Hsiang D, Butler J, Tromberg BJ. Monitoring neoadjuvant chemotherapy in breast cancer using quantitative diffuse optical spectroscopy: a case study. J Biomed Opt. 2004; 9(1):230–238. [PubMed: 14715078]
18. Wang J, Jiang S, Li Z, diFlorio-Alexander RM, Barth RJ, Kaufman PA, Pogue BW, Paulsen KD. In vivo quantitative imaging of normal and cancerous breast tissue using broadband diffuse optical tomography. Med Phys. 2010; 37(7):3715–3724. [PubMed: 20831079]
19. Flexman ML, Kim HK, Gunther JE, Lim Ea, Alvarez MC, Deperito E, Kalinsky K, Hershman DL, Hielscher AH. Optical biomarkers for breast cancer derived from dynamic diffuse optical tomography. J Biomed Opt. 2013; 18(9):96012.
20. Jiang S, Pogue BW, Carpenter CM, Poplack SP, Wells Wa, Kogel Ca, Forero Ja, Muffly LS, Schwartz GN, Paulsen KD, et al. Evaluation of breast tumor response to neoadjuvant chemotherapy with tomographic diffuse optical spectroscopy: case studies of tumor region-of-interest changes. Radiology. 2009; 252(2):551–560. [PubMed: 19508985]
21. Jiang S, Pogue BW, Kaufman Pa, Gui J, Jermyn M, Frazee TE, Poplack SP, DiFlorio-Alexander R, Wells Wa, Paulsen KD. Predicting Breast Tumor Response to Neoadjuvant Chemotherapy with Diffuse Optical Spectroscopic Tomography prior to Treatment. Clin Cancer Res. 2014; 20(23): 6006–6015. [PubMed: 25294916]
22. Choe R, Konecky SD, Corlu A, Lee K, Durduran T, Busch DR, Pathak S, Czerniecki BJ, Tchou J, Fraker DL, et al. Differentiation of benign and malignant breast tumors by in-vivo three-dimensional parallel-plate diffuse optical tomography. J Biomed Opt. 2009; 14(2):24020.
23. Grosenick D, Wabnitz H, Moesta KT, Mucke J, Schlag PM, Rinneberg H. Time-domain scanning optical mammography: II. Optical properties and tissue parameters of 87 carcinomas. Phys Med Biol. 2005; 50(11):2451–2468. [PubMed: 15901948]
24. Taroni P, Bassi A, Comelli D, Farina A, Cubeddu R, Pifferi A. Diffuse optical spectroscopy of breast tissue extended to 1100 nm. J Biomed Opt. 2012; 14(5):54030.
25. Fang Q, Selb J, Carp SA, Boverman G, Miller EL, Brooks DH, Moore RH, Kopans DB, Boas DA. Combined optical and x-ray tomosynthesis breast imaging. Radiology. 2010; 258(1):89–97. [PubMed: 21062924]
26. Soliman H, Gunasekara A, Rycroft M, Zubovits J, Dent R, Spayne J, Yaffe MJ, Czarnota GJ. Functional imaging using diffuse optical spectroscopy of neoadjuvant chemotherapy response in women with locally advanced breast cancer. Clin Cancer Res. 2010; 16(9):2605–2614. [PubMed: 20406836]
27. Falou O, Soliman H, Sadeghi-Naini A, Iradji S, Lemon-Wong S, Zubovits J, Spayne J, Dent R, Trudeau M, Boileau JF, et al. Diffuse optical spectroscopy evaluation of treatment response in women with locally advanced breast cancer receiving neoadjuvant chemotherapy. Transl Oncol. 2012; 5(4):238–246. [PubMed: 22937175]
28. Schaafsma BE, van de Giessen M, Charehbili A, Smit VTHBM, Kroep JR, Lelieveldt BPF, Liefers G-J, Chan A, Lowik CWGM, Dijkstra J, et al. Optical mammography using diffuse optical spectroscopy for monitoring tumor response to neoadjuvant chemotherapy in women with locally advanced breast cancer. Clin Cancer Res. 2015; 21(3):577–584. [PubMed: 25473002]

29. Rinneberg H, Grosenick D, Moesta KT, Wabnitz H, Mucke J, Wübbeler G, Macdonald R, Schlag PM. Detection and characterization of breast tumours by time-domain scanning optical mammography. Opto-Electronics Rev. 2008; 16(2):147–162.
30. Choe R, Corlu A, Lee K, Durduran T, Konecky SD, Grosicka-Koptyra M, Arridge SR, Czerniecki BJ, Fraker DL, DeMichele A, et al. Diffuse optical tomography of breast cancer during neoadjuvant chemotherapy: a case study with comparison to MRI. Med Phys. 2005; 32(4):1128–1139. [PubMed: 15895597]
31. Tromberg BJ, Cerussi A, Shah N, Compton M, Durkin A, Hsiang D, Butler J, Mehta R. Imaging in breast cancer: diffuse optics in breast cancer: detecting tumors in premenopausal women and monitoring neoadjuvant chemotherapy. Breast Cancer Res. 2005; 7(6):279–285. [PubMed: 16457705]
32. Zhou C, Choe R, Shah N, Durduran T, Yu G, Durkin A, Hsiang D, Mehta R, Butler J, Cerussi A, et al. Diffuse optical monitoring of blood flow and oxygenation in human breast cancer during early stages of neoadjuvant chemotherapy. J Biomed Opt. 2007; 12(5):51903.
33. Tran WT, Childs C, Chin L, Slodkowska E, Sannachi L, Tadayyon H, Watkins E, Wong SL, Curpen B, El Kaffas A, et al. Multiparametric monitoring of chemotherapy treatment response in locally advanced breast cancer using quantitative ultrasound and diffuse optical spectroscopy. Oncotarget. 2016; 7(15):19762–19780. [PubMed: 26942698]
34. Pakalniskis MG, Wells WA, Schwab MC, Froehlich HM, Jiang S, Li Z, Tosteson TD, Poplack SP, Kaufman PA, Pogue BW, et al. Tumor angiogenesis change estimated by using diffuse optical spectroscopic tomography: demonstrated correlation in women undergoing neoadjuvant chemotherapy for invasive breast cancer? Radiology. 2011; 259(2):365–374. [PubMed: 21406632]
35. Busch DR, Choe R, Rosen MA, Guo W, Durduran T, Feldman MD, Mies C, Czerniecki BJ, Tchou J, Demichele A, et al. Optical malignancy parameters for monitoring progression of breast cancer neoadjuvant chemotherapy. Biomed Opt Express. 2013; 4(1):105–121. [PubMed: 23304651]
36. Gunther JE, Lim E, Kim HK, Flexman ML, Zweck L, Arora S, Refice S, Brown M, Kalinsky K, Hershman D, et al. Combined dynamic and static optical tomography for prediction of treatment outcome in breast cancer patients. SPIE Proc. 2015:953811.
37. Tromberg BJ, Zhang Z, Leproux A, O'Sullivan TD, Cerussi AE, Carpenter PM, Mehta RS, Roblyer D, Yang W, Paulsen KD, et al. Predicting responses to neoadjuvant chemotherapy in breast cancer: ACRIN 6691 trial of diffuse optical spectroscopic imaging. Cancer Res. 2016; 76(20):5933–5944. [PubMed: 27527559]
38. Ueda S, Roblyer D, Cerussi A, Durkin A, Leproux A, Santoro Y, Xu S, O'Sullivan TD, Hsiang D, Mehta R, et al. Baseline tumor oxygen saturation correlates with a pathologic complete response in breast cancer patients undergoing neoadjuvant chemotherapy. Cancer Res. 2012; 72(17):4318–4328. [PubMed: 22777823]
39. Zhu Q, Wang L, Tannenbaum S, Ricci A, DeFusco P, Hegde P. Pathologic response prediction to neoadjuvant chemotherapy utilizing pretreatment near-infrared imaging parameters and tumor pathologic criteria. Breast Cancer Res. 2014; 16(5):456. [PubMed: 25349073]
40. Sajjadi AY, Isakoff SJ, Deng B, Singh B, Wanyo CM, Fang Q, Specht MC, Schapira L, Moy B, Bardia A, et al. Normalization of compression-induced hemodynamics in patients responding to neoadjuvant chemotherapy monitored by dynamic tomographic optical breast imaging (DTOBI). Biomed Opt Express. 2017; 8(2):555–569. [PubMed: 28270967]
41. Cerussi AE, Tanamai VW, Mehta RS, Hsiang D, Butler J, Tromberg BJ. Frequent Optical Imaging during Breast Cancer Neoadjuvant Chemotherapy Reveals Dynamic Tumor Physiology in an Individual Patient. Acad Radiol. 2010; 17(8):1031–1039. [PubMed: 20542448]
42. Anderson PG, Kainerstorfer JM, Sassaroli A, Krishnamurthy N, Homer MJ, Graham RA, Fantini S. Broadband optical mammography: chromophore concentration and hemoglobin saturation contrast in breast cancer. PLoS One. 2015; 10(3):e0117322. [PubMed: 25781469]
43. Ogston KN, Miller ID, Payne S, Hutcheon AW, Sarkar TK, Smith I, Schofield A, Heys SD. A new histological grading system to assess response of breast cancers to primary chemotherapy: Prognostic significance and survival. Breast. 2003; 12(5):320327.
44. Rodenhuis S, Mandjes IA, Wesseling J, van de Vijver MJ, Peeters MJ, Sonke GS, Linn SC. A simple system for grading the response of breast cancer to neoadjuvant chemotherapy. Ann Oncol. 2010; 21(3):481–487. [PubMed: 19717533]

45. Contini D, Martelli F, Zaccanti G. Photon migration through a turbid slab described by a model based on diffusion approximation I Theory. Appl Opt Optical Society of America. 1997; 36(19): 4587.
46. Anderson PG, Sassaroli A, Kainerstorfer JM, Krishnamurthy N, Fantini S. Broadband optical mammography: Breast tissue thickness compensation algorithm. Int Soc Opt Photonics. 2015:93190L.
47. Madsen K, Nielsen H, Tingleff O. Methods for Non-Linear Least Squares Problems. 2004
48. Prahl, S. Oregon Med. Laser Center; Portland, OR: 2002. Optical absorption of hemoglobin. http://omlc.org/spectra/hemoglobin/summary.html. Accessed October 10, 2015
49. Arridge SR, Lionheart WRB. Nonuniqueness in diffusion-based optical tomography. Opt Lett OSA. 1998; 23(11):882.
50. Groopman JE, Itri LM. Chemotherapy-induced anemia in adults: incidence and treatment. J Natl Cancer Inst. 1999; 91(19):1616–1634. [PubMed: 10511589]
51. O'Sullivan TD, Leproux A, Chen J-H, Bahri S, Matlock A, Roblyer D, McLaren CE, Chen W-P, Cerussi AE, Su M-Y, et al. Optical imaging correlates with magnetic resonance imaging breast density and reveals composition changes during neoadjuvant chemotherapy. Breast Cancer Res. 2013; 15(1):R14. [PubMed: 23433249]
52. Carraresi S, Shatir TS, Martelli F, Zaccanti G. Accuracy of a perturbation model to predict the effect of scattering and absorbing inhomogeneities on photon migration. Appl Opt. 2001; 40(25): 4622–4632. [PubMed: 18360503]
53. Duch J, Fuster D, Muñoz M, Fernández PL, Paredes P, Fontanillas M, Guzmán F, Rubí S, Lomeña FJ, Pons F. 18F-FDG PET/CT for early prediction of response to neoadjuvant chemotherapy in breast cancer. Eur J Nucl Med Mol Imaging. 2009; 36(10):1551–1557. [PubMed: 19326117]
54. Delille J, Slanetz P, Yeh E, Halpern E. Invasive Ductal Breast Carcinoma Response to Neoadjuvant Chemotherapy: Noninvasive Monitoring with Functional MR Imaging—Pilot Study 1. Radiology. 2003; 228(1):63–69. [PubMed: 12775851]
55. Pickles MD, Lowry M, Manton DJ, Gibbs P, Turnbull LW. Role of dynamic contrast enhanced MRI in monitoring early response of locally advanced breast cancer to neoadjuvant chemotherapy. Breast Cancer Res Treat. 2005; 91(1):1–10. [PubMed: 15868426]
56. Hayes C, Padhani AR, Leach MO. Assessing changes in tumour vascular function using dynamic contrast-enhanced magnetic resonance imaging. NMR Biomed. 2002; 15(2):154–163. [PubMed: 11870911]
57. Mankoff DA, Dunnwald LK, Gralow JR, Ellis GK, Schubert EK, Tseng J, Lawton TJ, Linden HM, Livingston RB. Changes in blood flow and metabolism in locally advanced breast cancer treated with neoadjuvant chemotherapy. J Nucl Med. 2003; 44(11):1806–1814. [PubMed: 14602864]
58. von Minckwitz G, Blohmer JU, Costa SD, Denkert C, Eidtmann H, Eiermann W, Gerber B, Hanusch C, Hilfrich J, Huober J, et al. Response-guided neoadjuvant chemotherapy for breast cancer. J Clin Oncol. 2013; 31(29):3623–3630. [PubMed: 24002511]

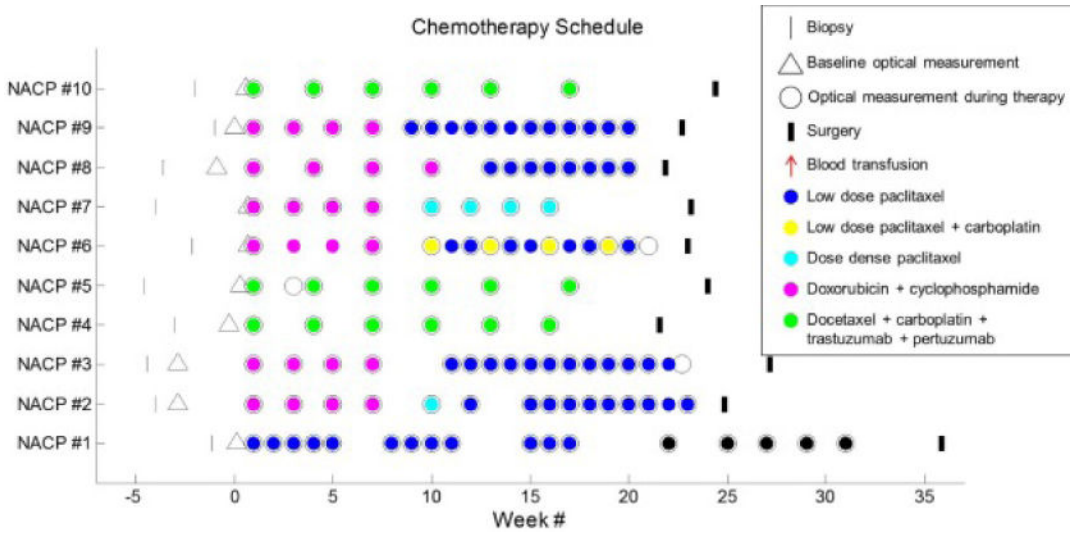

Figure 1.

Patients chemotherapy schedules. Week one corresponds to the first infusion time point. The times of biopsy, infusions, surgery, and blood transfusions are indicated for all ten patients. The type of drug administered is also indicated by the color within the chemotherapy infusion open circles. The baseline optical mammograms (open triangles) were obtained 2–27 days before the treatment began. The overlapping baseline optical mammogram point and first infusion point for NACP # 6, 7, and 10 indicate that these occurred 2 days within one another.

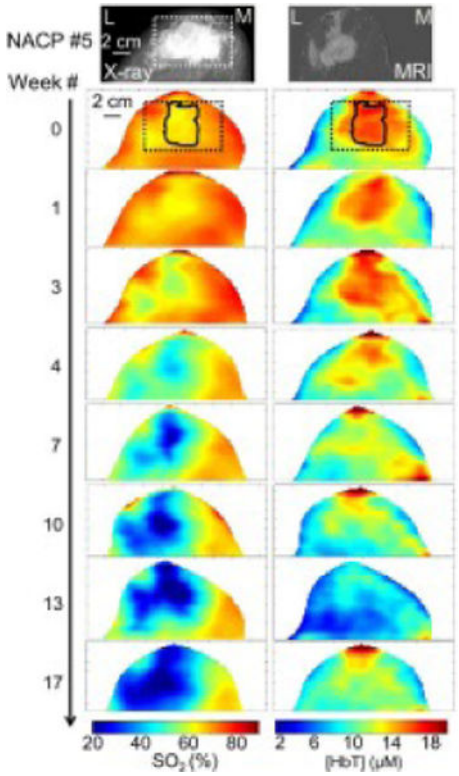

Figure 2.

Left breast images for NACP #5, an R (pCR) patient. In all images, the left side of each image is lateral (L) and the right side of each image is medial (M). The craniocaudal full-field digital mammogram (top left) depicts an irregular, partially spiculated mass (white box) located in the left breast corresponding to the patient's biopsy-proven malignancy, prior to treatment. The MRI axial contrast-enhanced subtraction image (top right) demonstrates a 4.4 cm irregular mass with additional areas of non-mass enhancement extending to the nipple and laterally. The optical [HbT] and SO_2 maps obtained throughout NAC show the progressive decrease of [HbT] and SO_2 at the cancerous region (identified at week 0 by the solid line within the dashed rectangle corresponding to the location of the mass visible in the X-ray image). Subsequent surgical specimen (not shown) revealed a pCR.

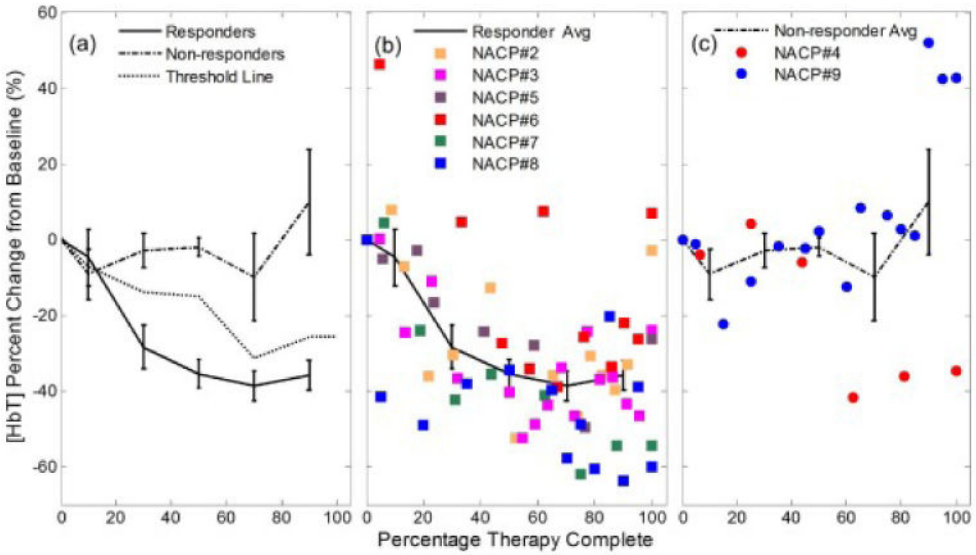

Figure 3.

(a) Trends of [HbT] at the tumor ROI for both response categories at a group level (the error bars represent the standard error). The threshold dashed line represents the weighted average of the mean percent changes of [HbT] for the R and NR groups using the inverse of the standard error as the weights.. This line is used for assessing patient response and is discussed in relation to the cumulative response index. The individual patient data throughout therapy are shown in (b) for responders and (c) for non-responders, along with the corresponding group average line.

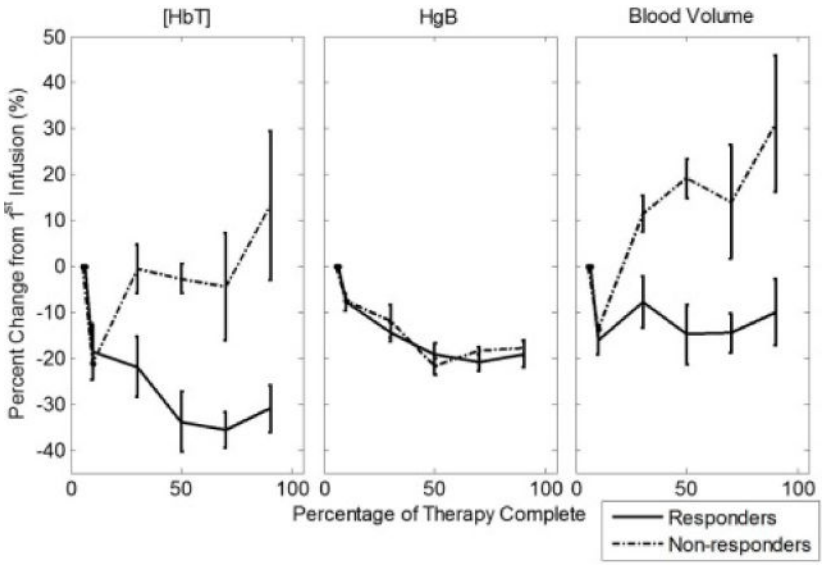

Figure 4.

Average change in blood volume, [HbT], and hemoglobin concentration in blood (Hgb) relative to the first infusion throughout chemotherapy for responders and non-responders. All patients show a similar systemic decrease in Hgb during NAC, but blood volume fraction in breast tissue decreases in responders and increases in non-responders.

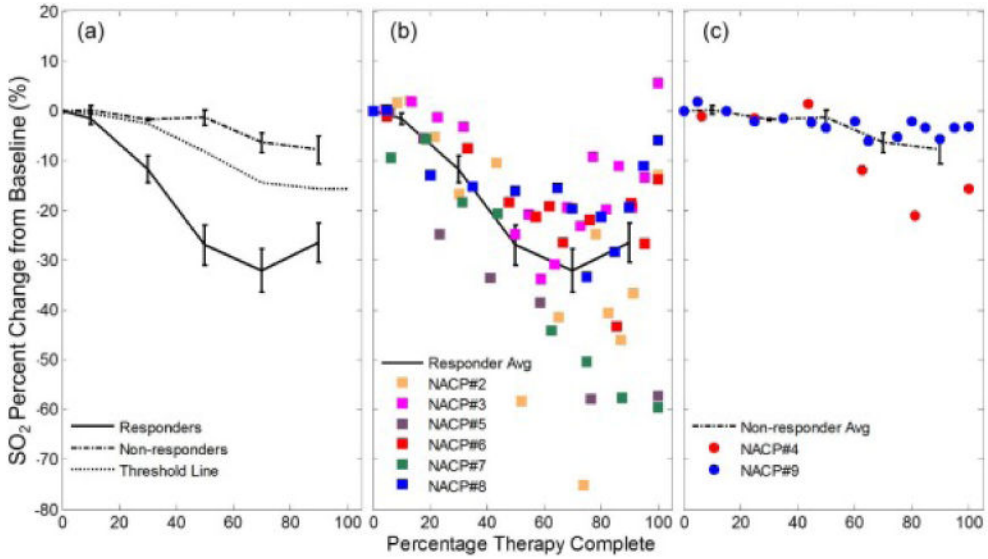

Figure 5.

(a) Trends of SO_2 at the tumor ROI for both response categories at a group level (the error bars represent the standard error). The threshold dashed line represents the weighted average of the mean percent changes of SO_2 for the R and NR groups using the inverse of the standard error as the weights. This line is used for assessing patient response and is discussed in relation to the cumulative response index. The individual patient data throughout therapy are shown in (b) for responders and (c) for non-responders, along with the corresponding group average line.

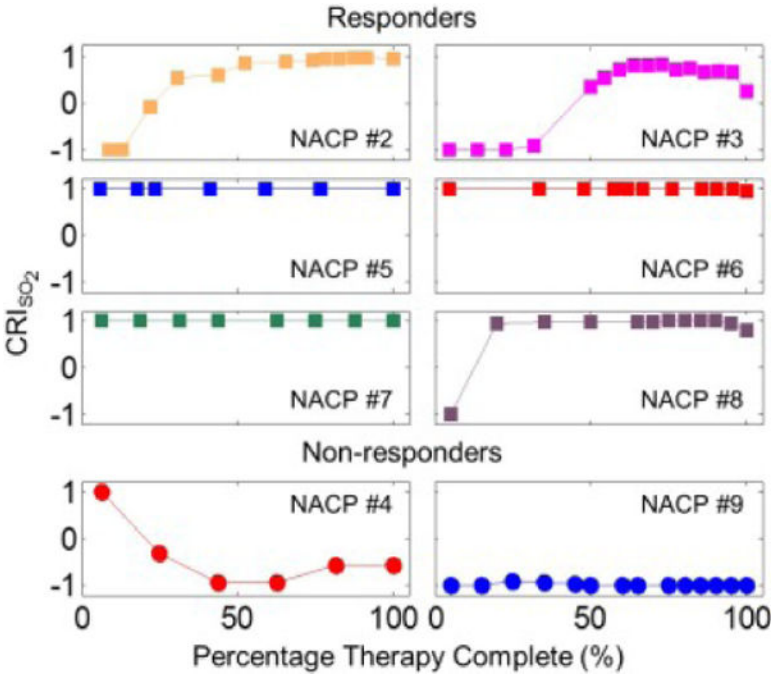

Figure 6.

Cumulative response index (CRI), based on SO_2 at the tumor ROI, for each individual patient throughout the course of neoadjuvant chemotherapy. The CRI can take values between −1 (poor response) and +1 (good response).

Table 1

Chronological summary of published studies of optical mammography on patients undergoing neoadjuvant breast cancer chemotherapy.

Reference	Year	# Subjects	# Sessions	Duration (weeks)	MAJOR FINDINGS
Jakubowski et al. [17]	2004	1	8	10	***After 1 week:*** ↓[HbT] (−26%) (PR) ***After 10 weeks:*** ↓[HbT] (−56%), ↓[H_2O](−67%), ↑SO_2 (PR) Similar trend in control tissue (breast, abdomen): ↓[HbO_2], →[Hb], ↓Hgb (−16%)
Choe et al. [30]	2005	1	3	24 (Entire NAC)	***Between 4th and 7th cycle:*** ↓[HbT] (−50%) (PR)
Tromberg et al. [31]	2005	1	6	1	***After 1 week:*** ↓TOI (−60%), ↓[HbT] (−30%), ↓[H_2O] (−30%), ↑[lipid] (+20%)
Cerussi et al. [12]	2007	11	2	1	***After 1 week:*** ↓[Hb] (−27%), ↓[HbO_2] (−33%), ↓[H_2O] (−11%) (responders) No change (NR and healthy tissue)
Zhou et al. [32]	2007	1	6	1	***After 1 week:*** ↓T/N [Hb] (−31%), ↓T/N [HbO_2] (−27%), ↓T/N [HbT] (−28%), ↑T/N [lipid] (+16%), ↓T/N Blood Flow (−25%) (PR)
Zhu et al. [13]	2008	11	3	Entire NAC	***After 2nd cycle:*** Lower BVI in complete responders vs. partial/non-responders ***At end of therapy:*** ↓BVI (−71%) (pCR), ↓BVI (−54%) (PR), ↓BVI (−13%) (NR)
Jiang et al. [20]	2009	7	5–11	Entire NAC	***Within week 4:*** ↓[HbT] (−64%) (pCR) ↑[HbT] (+17%) (non-pCR)
Soliman et al. [26]	2010	10	5	Entire NAC	***After 4 weeks:*** ↓[Hb] (−68%), ↓[HbO_2] (−59%), ↓[H_2O] (−51%), ↓SP (−53%) (pCR, PR) ↓[Hb] (−18%), ↓[HbO_2] (−18%), ↓[H_2O] (−15%), ↓SP (−13%) (NR)
Cerussi et al. [41]	2010	1	19	18 (Entire NAC)	↓T/N TOI ratio throughout NAC (−50% at end of therapy)
Roblyer et al. [14]	2011	23	8	1	***After 1 day:*** ↑[HbO_2] (+41%, +44%) (pCR, PR), ↓[HbO_2] (−22%) (NR) ***After 1 week:*** ↓[HbO_2] (−22%) (pCR), →[HbO_2] (PR), ↓[HbO_2] (−49%) (NR)
Cerussi et al. [15]	2011	34	3	Entire NAC	***At therapy midpoint:*** ↓T/N TOI: −47% (pCR), −20% (non-pCR)
Pakalniskis et al. [34]	2011	11	3	Entire NAC	***During therapy:*** ↓[HbT] (10%/month) (pCR), →[HbT] (PR)
Falou et al. [27]	2012	15	5	Entire NAC	***After 1 week:*** ↑[Hb] (17%), ↑[HbO_2] (8%), ↑[HbT] (10%), ↑[H_2O] (11%) (responders) ↓[Hb] (−14%), ↓[HbO_2] (−18%), ↓[HbT] (−17%), ↓[H_2O] (−29%) (NR)
Ueda et al. [38]	2012	41	1	Baseline only	***Before treatment:*** Tumor [Hb], [HbO_2], [HbT] did not correlate with response Tumor StO_2 was higher in pCR (78%) than in non-pCR (72%)
Busch et al. [35]	2013	30	2–4	Entire NAC	Initial test of a statistical analysis of [HbT], SO_2, μ_s' images to extract a predictive parameter of NAC response
Zhu et al. [16]	2013	32	4	Entire NAC	***Before treatment:*** Greater pretreatment [HbT] in responders than non-responders ***After 1st cycle:*** ↓[HbT] (−12%) (CR); →[HbT] (PR, NR)
Zhu et al. [39]	2014	34	1	Baseline only	***Before treatment:*** Tumor pretreatment [HbT] is best predictor of NAC response
Jiang et al. [21]	2014	19	3	Entire NAC	***Before treatment:*** Greater pretreatment [HbT] in pCR than in non-pCR ***By the end of 1st cycle:*** ↓[HbT] (−43%) (pCR); ↑[HbT] (+20%) (PR)
Schaafsma et al. [28]	2015	22	4	Entire NAC	***After 1st cycle (3 weeks):*** ↓[HbO_2] (−14%), (pCR, PR); ↑[HbO_2] (+36%), (NR)

Reference	Year	# Subjects	# Sessions	Duration (weeks)	MAJOR FINDINGS
					After 3rd cycle (9 weeks, therapy midpoint): ↓[HbO_2] (−32%), (pCR, PR); ↑[HbO_2] (+10%), (NR)
Gunther et al. [36]	2015	22	2	2	***After 2 weeks:*** ↓[HbT] (−35%) (pCR), ↓[HbT] (−5%) (PR), ↑[HbT] (+5%) (NR) Faster breath-hold washout rate of [Hb] in pCR vs. non-pCR
Tran et al. [33]	2016	22	5	Entire NAC	***After 1 week:*** Combination of tumor ↓[HbT] and Quantitative Ultrasound parameters resulted in perfect markers for response
Tromberg et al. [37]	2016	34	4	Entire NAC	***At therapy midpoint:*** ↓T/N TOI: −46% (pCR), −14% (non-pCR)
Sajjadi et al. [40]	2017	13	2–3	4	***After 4 weeks:*** Different T/N breast compression dynamics of [HbT] and SO_2 in CR&PR vs. NR
This work	2017	8	7–18	18–22 (Entire NAC)	***At therapy midpoint:*** ↓[HbT] (−35%), ↓SO_2 (−27%) (pCR & PR) →[HbT], →SO_2 (NR)

NAC: neoadjuvant chemotherapy; TOI: tissue optical index ([Hb]×[H_2O]/[lipid]); BVI: blood volume index ([HbT]×TV, with TV tumor volume); SP: scattering power; T/N: tumor-to-normal ratio; pCR: pathologic complete responders; CR, PR, NR: complete, partial, non-responders. ↓, ↑, and → indicate a decrease, increase, and no change, respectively.

Table 2

Patient details and treatment regimens.

NACP #	Ref. #	Age (yr)	Pre-treatment cancer size (cm)		Cancer stage	Cancer subtype	Chemotherapy agent	Infusion Frequency (number)	Treatment duration (weeks)	Post-treatment cancer size (Hist.) (cm)	NAC response
			MRI X-ray	Optical							
1	164	38	9.4	1.2	IIIC	ER+/HER2−	Paclitaxel	Weekly (12)	31	6.0	NR (PR2)
							Capecitabine	Bi-weekly (5)			
2	163	72	3.2	2.1	IIB	TNBC	Doxorubicin, Cyclophosphamide	Bi-weekly (4)	23	–	R (pCR)
							Paclitaxel	Weekly (12)			
3	165	57	2.5	1.4	IIB	ER+/HER2−	Doxorubicin, Cyclophosphamide	Bi-weekly (4)	22	0.9	R (PR1)
							Paclitaxel	Weekly (12)			
4	166	54	2.9	1.3	IIIA	HER2+	Carboplatin, Docetaxel, Trastuzumab, Pertuzumab	Every 3 weeks (6)	16	2.8	NR (PR2)
5	167	46	4.4	3.7	IV	HER2+	Carboplatin, Docetaxel, Trastuzumab, Pertuzumab	Every 3 weeks (6)	17	–	R (pCR)
6	168	47	6.0	4.4	IIB	TNBC	Doxorubicin, Cyclophosphamide	Bi-weekly (4)	21	0.4	R (PR1)
							Paclitaxel w/Carboplatin (every 3rd)	Weekly (11)			
7	169	44	7.0	3.5	IIIA	ER+/HER2−	Doxorubicin, Cyclophosphamide	Bi-weekly (4)	16	0.6	R (PR1)
							Paclitaxel	Bi-weekly (4)			
8	170	74	Inflam	2.6	IIIB	ER+/HER2−	Doxorubicin, Cyclophosphamide	Every 3 weeks (4)	20	1.7	R (PR1)
							Paclitaxel	Weekly (8)			
9	171	44	Inflam	1.3	IIIB	ER+/HER2−	Doxorubicin, Cyclophosphamide	Bi-weekly (4)	20	11.3	NR (PR2)
							Paclitaxel	Weekly(12)			
10	173	56	4.5	1.9	IIB	HER2+	Carboplatin, Docetaxel, Trastuzumab, Pertuzumab	Every 3 weeks (6)	17	–	R (pCR)

Note - Ref #: progressive patient number; Age: age of patient at time of baseline scan; Pretreatment cancer size: maximum tumor dimension pretreatment (one column reports the dimension from MRI or full-field digital mammography, one column reports the size of the tumor ROI from optical mammography), “Inflam” denotes inflammatory breast cancer; Cancer stage: initial clinical cancer stage; Cancer subtype: triple-negative breast cancer (TNBC), estrogen-receptor-positive/progesterone-receptor-negative (ER+/HER2−), and HER2+; Chemotherapy agent: chemotherapy drugs administered to patient; Infusion frequency (total number): how often infusions were performed (and total number of infusions); Duration of treatment: how long the patients underwent treatment (including breaks in therapy schedule); Post-treatment cancer size (Hist.): maximum tumor dimension post treatment from histology after surgical resection; Response level: individual patient’s response (R: responder showing either a pathologic complete response (pCR) [no remaining tumor] or partial response 1 (PR1) [tumor decreased by more than 50% in size]; NR: non-responder showing partial response 2 (PR2) [tumor decreased by less than 50% in size]).

Table 3

Summary of the means and standard errors of relative changes in [Hb], [HbO_2], [HbT], and SO_2 at the tumor region of interest from baseline over 5 binned time windows for each response category. Beneath the response category, the number of patients in each group (*n*) is also provided.

		Response to therapy at the tumor ROI (% change from baseline)			
Group	**Percent therapy complete**	**[Hb]**	**[HbO_2]**	**[HbT]**	**SO_2**
Responders (*n* = 6)	10 (0, 20]	−2 ± 8	−6 ± 7	−5 ± 7	−2 ± 1
	30 (20, 40]	−13 ± 7	−36 ± 6	−28 ± 6	−12 ± 3
	50 (40, 60]	−4 ± 5	−52 ± 5	−35 ± 4	−27 ± 4
	70 (60, 80]	−4 ± 6	−56 ± 5	−38 ± 4	−32 ± 4
	90 (80, 100]	4 ± 7	−52 ± 4	−36 ± 4	−26 ± 4
Non-responders (*n* = 2)	10 (0, 20]	−9 ± 7	−9 ± 7	−9 ± 7	0 ± 1
	30 (20, 40]	1 ± 4	−5 ± 4	−3 ± 4	−2 ± 0
	50 (40, 60]	1 ± 5	−3 ± 1	−2 ± 2	−1 ± 1
	70 (60, 80]	0 ± 11	−15 ± 12	−10 ± 12	−6 ± 2
	90 (80, 100]	23 ± 12	3 ± 15	10 ± 14	−8 ± 3

Table 4

Predictive values of the NAC response assessment based on changes from baseline (*p* values) and CRI (sensitivity and specificity) from [HbT], SO_2, [Hb], and $[HbO_2]$ measurements at the tumor ROI for each time bin.

% Therapy Complete	% Change from Baseline				Cumulative Response Index (CRI)			
	[HbT]	SO_2	[Hb]	$[HbO_2]$	[HbT]	SO_2	[Hb]	$[HbO_2]$
	p value	*p* value	*p* value	*p* value	Sens/Spec	Sens/Spec	Sens/Spec	Sens/Spec
10 (0, 20]	0.9	0.8	0.6	1	0.33/1	0.5/0.5	0.33/0.5	0.5/0.5
30 (20, 40]	0.06	0.06	0.2	0.06	0.67/0.5	0.83/1	0.67/0.5	0.83/1
50 (40, 60]	0.01	0.01	0.46	0.01	0.83/1	1/1	0.67/0	0.83/1
70 (60, 80]	0.05	0.002	0.6	0.02	0.83/1	1/1	0.67/0.5	1/1
90 (80, 100]	0.01	0.01	0.14	0.004	1/0.5	1/1	0.5/0.5	1/1